

# FEATURE EXTRACTION OF EEG SIGNALS IN THE TIME-FREQUENCY DOMAIN OF REHABILITATION TASK FOR MOTOR IMAGERY BRAIN-COMPUTER INTERFACE IN UPPER LIMBS

DAINIER GONZÁLEZ ROMERO<sup>1</sup>, NUÑEZ CUELLAR SEBASTIAN<sup>2</sup>, NIETO VALENZUELA SERGIO ALEJANDRO<sup>2</sup>, RUTHBER RODRÍGUEZ SERREZUELA<sup>2</sup>, ENRIQUE MARAÑÓN REYES<sup>3</sup>, ARQUÍMEDES MONTOYA PEDRÓN<sup>4</sup>, ROBERTO SAGARÓ ZAMORA<sup>5</sup>

<sup>1</sup>Empresa de Telecomunicaciones de Cuba. División Territorial Santiago de Cuba. Departamento de Coordinación General. Santiago de Cuba, Cuba

<sup>2</sup>Corporación Universitaria del Huila, Neiva. Huila, Colombia

<sup>3</sup>Universidad de Oriente. Centro de Procesamiento de Imágenes y Señales, Facultad de Ingenierías en Telecomunicaciones, Informática y Biomédica. Santiago de Cuba, Cuba

<sup>4</sup>Hospital General “Dr. Juan Bruno Zayas”. Santiago de Cuba, Cuba

<sup>5</sup>Universidad de Oriente. Facultad de Ingeniería Mecánica e Industrial, Departamento de Mecánica y Diseño. Santiago de Cuba, Cuba

## ABSTRACT

Effective feature extraction and classification methods of electroencephalogram (EEG) signals are critical for enhancing the recognition accuracy of Brain-Computer Interface (BCI) systems used in disability assistive devices and rehabilitation equipment. This study aims to identify and integrate EEG signals that classify real and motor imagination (IM) movements within a BCI system for use in robotic technology in post-stroke patient rehabilitation. We propose a processing method that combines low and high pass filtering, principal component analysis (PCA), and time-frequency domain signal processing using the Fourier Transform. Signals were recorded from healthy subjects and synchronized with recording software via a custom interface, focusing on alpha and beta brain rhythms. After filtering, PCA was used to reduce the number of reading channels for each rhythm. A primary challenge addressed is the inconsistency in registering real and motor imagination movements based on EEG signals. Our methodology includes developing a visual interface using Matlab 2019 and the Neuronic Cognitive Stimulator to guide users through movement tasks while synchronizing and recording EEG data. Bandpass filters for alpha, mu, and beta rhythms were designed, with the Butterworth filter chosen for its optimal balance of performance and computational cost. PCA identified the most relevant EEG channels, reducing data dimensionality while preserving critical information. Fourier and Fast Fourier Transforms (FFT) were applied to differentiate movements based on frequency analysis. This approach successfully identified a fundamental frequency one second before movement execution, facilitating the recognition of movement intention. The developed system shows promise for improving the precision of BCI applications in neurorehabilitation, providing a flexible tool that can incorporate other signal extraction methods.

**Keywords:** *Feature extraction, principal components analysis, EEG signals.*

## 1. INTRODUCTION

The World Health Organization (WHO) estimates that over one billion people globally live with some form of disability, with nearly 200 million experiencing significant difficulties in daily

activities [1,2]. The increasing prevalence of disability, exacerbated by an aging population and the rise in chronic diseases, is a growing concern. Cerebrovascular accidents (CVA), a leading cause of death and motor disability, particularly alarm international health organizations [3-5]. Annually,

approximately 15 million individuals suffer from CVAs, resulting in 5 million deaths and another 5 million cases of permanent disability. Of these survivors, 50-70% experience sequelae, with about one-third unable to independently perform daily activities and 75% unable to return to work. Neurorehabilitation, as defined by WHO, is an active process aimed at achieving the best possible physical, mental, and social recovery for individuals with neurological injuries or diseases, facilitating their integration into their environment. This process involves restoring lost physical capacities to acceptable levels, re-training motor skills, improving posture, re-educating locomotion patterns, and positively influencing personality traits affected by neurological conditions.

In the last two decades, rehabilitation robotics has emerged with the aim of applying medical technologies that allow partial or total recovery of patients. In this context, mechatronic exoskeletons to support the motor recovery functions of patients [6] are one of the most promising technologies.

The BCI systems process the spontaneous EEG, as well as the evoked responses to stimuli delimited in time under different conditions to control external devices according to Vidal [7]. Wolpaw et al., conceptualize it as those systems that "provide the brain with a new channel of communication and non-muscular control" [8]. More recently, Kleber and Birbaumer adapted this definition to highlight its utility in alternative communication devices, by "...allowing users to send messages and instructions to the outside world without using their muscles" [9]. Its main applications result in those intended for clinical practice, where the use of BCI systems allows the control of robotic prostheses, wheelchairs, communication systems or motor rehabilitation control systems [10-12].

Universidad de Oriente has developed several prototypes of exoskeletons for the rehabilitation of the upper limb in hemiplegic patients in Cuba, one of which, operating in passive mode, has showed very favorable rates in hemiplegic patients suffering from painful shoulder syndrome with respect to the conventional therapies, and among those mentioned: greater range of joint movement, early elimination of pain, decreased spasticity and an increase in muscle tone.

One of the most important obstacles is the inconsistency of the registers of real movements and motor imagination based on EEG signals and their characteristics, which are far from being those incorporated into rehabilitation routines, and which,

as part of a BCI system, could later be part of the control of self-assisted therapy technologies.

The objective of this research is to identify and integrate EEG signals into a database that allows

classifying real movements and motor imagination for use in robotic technology incorporated in the rehabilitation process in post-stroke patients.

## 2. MATERIALS AND METHODS

Figure 1 shows the methodology proposed by the authors. Bottom, and 1.25cm from left and right, leaving a gutter width of 0.2 between columns.

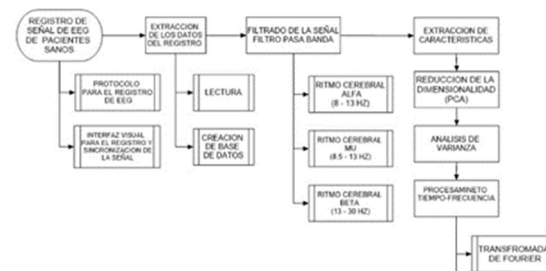


Figure 1: Proposed Methodology For The Extraction Of Characteristics Of EEG Signals Produced By Real Movements And Motor Imagination (MI) In Upper Limbs.

Based on a previous protocol inclusive of sample selection criteria (inclusion, exclusion and exit). The study sample was selected from a group of 10 healthy subjects who met the selection criteria. The movements to be executed by the subjects involved in the study were: shoulder flexion-extension, extension and abduction. Each subject performed a number of 10 repetitions of each exercise.



Figure 2: Movements Selected And Presented In The User Interface That Provides Information About Each Of The Movements In Addition To Controlling Their Execution.

**Inclusion criteria:** Adults in the age range of 18 - 30 years, with no history of Neurological and/or Psychiatric diseases were selected. They expressed their voluntary participation in the study, through verbal and written consent, and their subsequent acceptance by the work team in the Neurophysiology and Physiotherapy room at Juan Bruno Zayas Clinical Surgical Hospital.

**Exclusion:** cognitive, sensory, sensory, or communication deficits; pain, motor deficit and/or previous diagnosis of a musculoskeletal disorder of the shoulder.

**Exit Criteria:** voluntary abandonment, clinical complications which interfered the continuity of the study and/or treatment, absence from registration sessions and death.

## 2.1 User Interface

For the preparation of the user interface, the GUI tools of Matlab 2019<sup>a</sup> and the Neuronic Cognitive Stimulator were used as tools, which allowed the synchronization of the signal at the moment in which the subjects performed each of the movements between both applications. The latter makes it possible to synchronize the stimulation process with the recording of the electroencephalogram (EEG) and with the obtaining of functional magnetic resonance images (fMRI). In addition, it communicates through the serial port or the parallel port with the recording system to send marks synchronized with the appearance of stimuli and the subject's responses, recording the type of response, hit percentage and reaction time. EEG sampling was performed using the MEDICID 5 (N\_E 8.5) equipment (Figure 3) and the International System or Protocol 10-20 [13] was used for this purpose.



Figure 3: MEDICID 5 Equipment (N\_E 8.5), Sampling Frequency 200 HZ, 19 Monopolar EEG Channels, Input Range (V Min. -V Max.): 0.5 - 1. Npp At 5.0 Mvpp, High-Pass Filter: 0.5 Hz, Pass Filter Bass: 70hz

## 2.2 Principal Component Analysis (PCA)

When dealing with extensive datasets, signal processing becomes highly complex, necessitating the use of algorithms that reduce the dimensionality of these observations without losing critical information. This reduction facilitates the recognition of patterns within the signals. In this study, Principal Component Analysis (PCA), a widely employed unsupervised data extraction technique, was utilized [14-16]. PCA examines the variance-covariance structure among the variables in the input data, which include various observations described by multiple independent or dependent variables.

The application of PCA in this research was not intended to create a new lower-dimensional space by projecting the input data onto the directions of maximum variance. Instead, the goal was to identify the most relevant channels or electrodes. By focusing on the linear combination of variables with maximum variability, components with less variance were easily eliminated, ensuring minimal information loss.

## 2.3 Fourier Transform

Brain signal feature extraction translates the input brain signal into a vector of features correlated with the neurological phenomena associated with the signal [10]. This process is intricately tied to the acquisition system and represents the most complex aspect of BCI design, aiming to enhance the speed and precision of existing systems [17]. Several factors must be considered when acquiring brain activity information. First, artifacts—electrical signals present in the EEG that do not originate from brain activity—must be accounted for [18, 19]. Second, the non-stationary nature of EEG activity complicates the analysis [20, 21]. Third, temporal differences in the signal require careful handling.

The Fourier Transform (FT) is a widely used tool for signal processing, applicable in fields such as sound processing, biomedical signals, image processing, and EEG analysis. FT is particularly valued in EEG processing because it allows the analysis of signals from a frequency perspective, with the amplitude of each band (cerebral rhythm) reflecting the type of brain processing occurring. Given the discretized nature of EEG data in medical applications and the finite time of signal acquisition, the Discrete Fourier Transform (DFT) is used. However, due to the significant computational cost of DFT, efficient algorithms have been developed to calculate it, known collectively as the Fast Fourier

Transform (FFT). The Discrete Fourier Transform (DTF) and the Fast Fourier Transform (FFT) were used in this research.

### 3. RESULTS

#### 3.1 Visual Interface With 2019<sup>a</sup> and Neuronic Cognitive Stimulator

Every time the user has accessed the user interface (figure 2) and the movement to be executed has been selected, the user will receive graphical information on the movement to be carried out in a new window and will be guided on the start and end of each movement. (Figure 4).

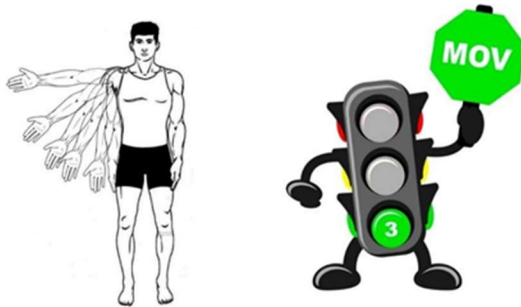


Figure 4: Execution Of The Abduction-Adduction Movement.

When starting the simulation, while the exercises are displayed through these animated images, synchronism marks (states) of start, stop, start and end of repetition of each exercise are sent, through the serial port connection of the display computer and the reading and recording computer (Figure 5).

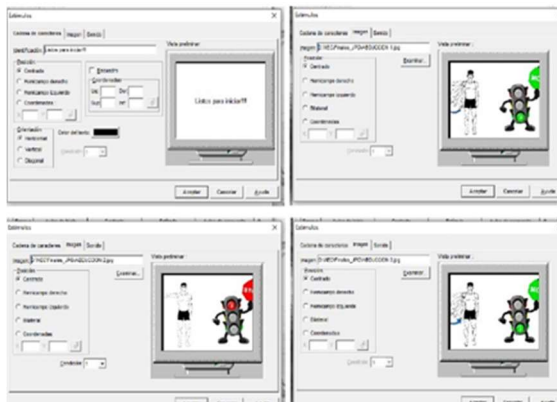


Figure 5: Configuration Of States In The Visual Interface With The Neuronic Cognitive Stimulator.

From the synchronization with the Neuronic Cognitive Stimulator detects the start,

stop, start and stop of each exercise for further processing (Figure 6).



Figure 6: Registration results with the Visual Interface of the Cognitive Stimulator

Due to the execution times of each movement and the post-interval time configured in the Cognitive Stimulator, it is possible to identify which movement is executed. The total duration of bursts among each group of repetitions, the duration of each repetition, was counted, and thus it was possible to identify which exercise had been executed, then place the repetitions of each exercise in variables in a different way, grouped into movements (Figure 7).

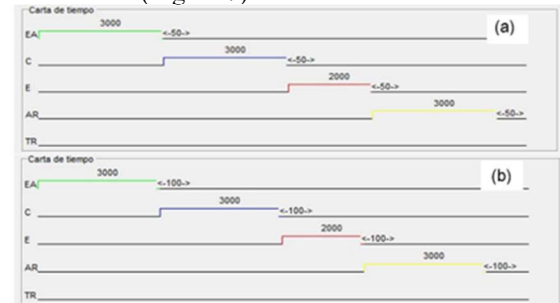


Figure 7: Timecards. (A) Abduction-Adduction (EA: 3000 Ms, C: 3000 Ms, E: 2000 Ms, AR: 3000 Ms, Post Interval In Each Exercise: 50 Ms). (B) Flexion-Extension (EA: 3000 Ms, C: 2000 Ms, E: 2000 Ms, AR: 3000 Ms, Post Interval In Each Exercise: 100 Ms).

As mentioned, making use of the interface made with Matlab 2019 and the Neuronic Cognitive Stimulator leaves synchrony marks, and for its subsequent processing and analysis, it was necessary to convert these synchrony marks into state marks, by editing each of the files resulting from the reading with the recording software used, which in that case was Neuronic Analysis of Psychophysiology. A tool that allows the modification of each of these extension files: .MRK, .PLG, .INF, .PAT. (Figure 8).



Figure 8: Conversion Of Sync Marks To Status Marks To The Files Resulting From The Record

### 3.2 EEG Signals

Bandpass filters were designed at the frequencies of the alpha (8 - 13 Hz), mu (8.5 - 13 Hz) and beta (13 -30 Hz) brain rhythms, which are directly involved with mental concentration, performing movements, tactile and visual stimuli, and even with the imagination or preparation of a movement.

A script that allowed comparing 4 types of filters (Butterworth, Chebyshev Type I, Chebyshev Type II and Elliptical) low-pass infinite impulse response (IIR), all 5th order, with a cutoff frequency of 2GHz was developed with the use of Matlab. In the cases of Chebyshev Type I, with an attenuation in the ripple band of 3dB, in the Chebyshev Type II with an attenuation of 30dB in the rejection band, and in the elliptical an attenuation of 3dB in the band ripple and 30dB in the rejection band.

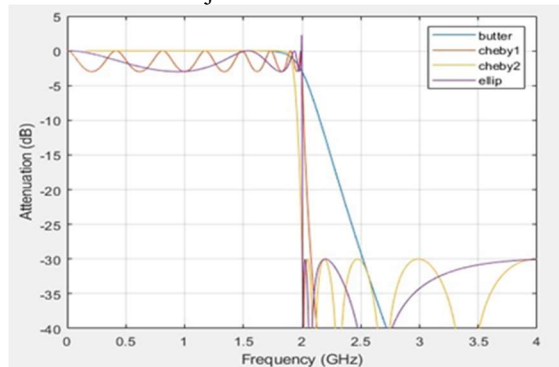


Figure 9: Graph Of Attenuation (Db) Vs. Frequency (Ghz)

As can be seen, in the Butterworth filter the transition band is less abrupt than in the other filters, however, it does not have ripple in the pass band or in the rejection band, while in the other filters it does present them (creating lobes side), which means that the response is not completely flat in the pass band, and if there are frequencies in the signal to be filtered at the frequencies of these lobes, these signals will be attenuated, but not in their entirety. Despite this, the Butterworth filter requires a higher computational cost than the other types of filters, it presents a phase closer to the ideal for a given order, but the order it needs to meet the specifications is usually significantly higher than that required by the others.

Of the remaining filters, the least complex is the elliptical one, but the latter has a peculiarity, and that is that its phase is the one that is furthest from linear behavior. It was decided to use a Butterworth filter [23] (Figure 9) when analyzing their response.

Depending on the brain rhythm, it corresponds to the frequencies of the pass and

rejection bands. In the case of the attenuation of the ripple in the pass band, 1 dB was chosen and the ripple in the rejection band 30dB. The order of filter 15 was chosen for our design after an analysis and comparison. (Figure 10).

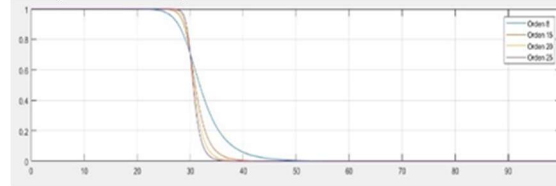


Figure 10: Comparison Of The Response Butterworth Filters Different Orders Figure 11 Shows The EEG Signal Recordings For The Abduction Movement, Unfiltered And Then Processed For The Different Bands.

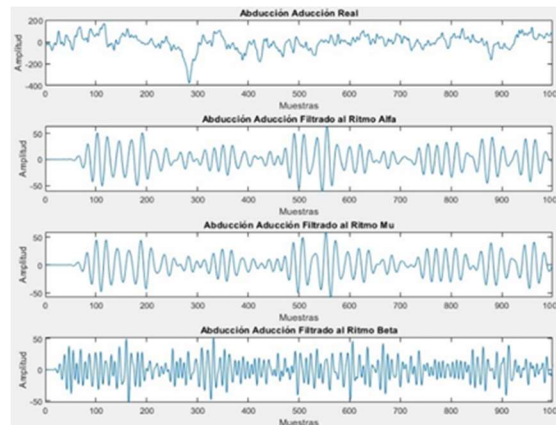


Figure 11: Cx Electrode Of The Exercise Abduction Adduction Filtered In Alpha, Mu And Beta Brain Rhythms.

### 3.3 Principal Component Analysis (PCA)

The acquired signal has 19 channels (variables) and more than a thousand observations, in addition to being filtered at the frequency of the 3 brain rhythms (Alpha, Mu and Beta) relevant to use in this study. Matlab 2019 software was used for the application of the principal component analysis method in this work, which has the PCA function. Regarding the present research, calculating the main components until obtaining a 95% explanation of the variability of the data was chosen. As such, up to the 12th CP's were analyzed for each movement, and each one of the brain rhythms, since in some cases in the 10th CP's the % explanation of variability had already been met, but in other cases it was only achieved in the 12th CP's.

Tables 1 and 2 show the results obtained for patient 22DGR, in performing the first movement at the frequency of the alpha brain rhythm.

It is observed in this case that to obtain a 95% explanation of data variability, which is sufficient with the first 10 components (1st CP:

32.2%, 2nd CP:20.78%, 3rd CP:14.10%, ....., 10th PC:1.48% Total: 95.07%).

Table 1: Eigenvalue Matrix

	PC1	PC2	PC3	PC4	PC5	PC6	PC7	PC8	CP9	PC10	PC11	PC12
FP1	-0.22	0.09	0.20	-0.19	-0.34	-0.26	0.23	0.41	0.33	0.14	-0.04	-0.22
FP2	-0.20	0.00	0.21	-0.26	-0.03	-0.21	0.18	0.10	-0.11	0.19	-0.05	0.26
F3	-0.22	0.06	-0.04	0.03	-0.25	0.15	-0.06	-0.06	0.20	-0.51	-0.20	-0.19
F4	-0.21	-0.08	0.09	-0.22	0.09	-0.01	0.02	0.00	-0.16	-0.08	0.03	0.38
C3	-0.09	0.12	-0.29	0.42	-0.22	0.12	0.15	-0.25	0.13	0.12	-0.48	0.16
C4	-0.03	-0.35	-0.08	0.21	0.37	-0.36	-0.30	0.01	0.59	-0.02	0.08	0.24
P3	0.22	0.19	-0.45	0.07	0.02	-0.20	0.54	-0.01	-0.10	-0.14	0.20	0.26
P4	0.34	-0.42	-0.14	0.06	-0.24	-0.35	-0.15	0.24	-0.40	-0.30	-0.05	-0.21
O1	0.34	0.30	-0.13	-0.40	0.26	0.04	0.09	-0.16	0.29	-0.13	0.21	-0.29
o2	0.47	-0.15	0.04	-0.38	-0.36	0.18	-0.25	-0.28	0.11	0.28	-0.19	0.20
F7	-0.13	0.20	0.13	0.14	-0.26	-0.08	-0.15	-0.12	0.03	0.01	0.22	-0.19
F8	-0.11	-0.04	0.25	-0.08	0.20	-0.18	0.12	-0.34	-0.27	0.08	-0.12	0.01
T3	-0.03	0.32	0.07	0.29	-0.20	-0.05	-0.35	-0.14	-0.17	0.12	0.54	0.12
T4	0.00	-0.08	0.31	0.16	0.29	-0.08	0.12	-0.39	-0.11	-0.08	-0.15	-0.37
T5	0.18	0.50	0.04	0.06	0.34	0.00	-0.35	0.44	-0.17	0.04	-0.42	0.04
T6	0.34	-0.18	0.46	0.35	0.03	0.45	0.32	0.29	0.10	-0.01	0.16	0.10
Fz	-0.26	-0.10	-0.08	-0.19	0.05	0.31	-0.10	0.06	-0.09	-0.30	0.10	0.18
Cz	-0.24	-0.17	-0.23	-0.12	0.14	0.41	-0.09	0.09	-0.09	0.00	0.10	-0.12
Pz	-0.12	-0.20	-0.35	0.06	0.12	0.11	0.04	0.12	-0.10	0.58	0.07	-0.36

Table 2: Matrix Of Eigenvectors And Accumulated.

	Eigenvector	%	Accumulated
PC1	5.80	32.20	32.20
PC2	3.74	20.78	52.98
PC3	2.54	14.10	67.07
PC4	1.20	6.67	73.74
PC5	1.14	6.34	80.08
PC6	0.88	4.89	84.97
PC7	0.72	3.99	88.96
PC8	0.50	2.78	91.74
CP9	0.33	1.85	93.59
PC10	0.27	1.48	95.07
PC11	0.23	1.27	96.34
PC12	0.21	1.16	97.50

The absolute value of each of the coefficients is determined to establish which channels are relevant, and then the central or average value of each of the coefficients from each principal component is calculated (Table 3).

Table 3: Matrix Of Absolute Eigenvalues.

	PC1	PC2	PC3	PC4	PC5	PC6	PC7	PC8	CP9	PC10	PC11	PC12
FP1	0.22	0.09	0.20	0.19	0.34	0.26	0.23	0.41	0.33	0.14	0.04	0.22
FP2	0.20	0.00	0.21	0.26	0.03	0.21	0.18	0.10	0.11	0.19	0.05	0.26
F3	0.22	0.06	0.04	0.03	0.25	0.15	0.06	0.06	0.20	0.51	0.20	0.19
F4	0.21	0.08	0.09	0.22	0.09	0.01	0.02	0.00	0.16	0.08	0.03	0.38
C3	0.09	0.12	0.29	0.42	0.22	0.12	0.15	0.25	0.13	0.12	0.48	0.16
C4	0.03	0.35	0.08	0.21	0.37	0.36	0.30	0.01	0.59	0.02	0.08	0.24
P3	0.22	0.19	0.45	0.07	0.02	0.20	0.54	0.01	0.10	0.14	0.20	0.26
P4	0.34	0.42	0.14	0.06	0.24	0.35	0.15	0.24	0.40	0.30	0.05	0.21
O1	0.34	0.30	0.13	0.40	0.26	0.04	0.09	0.16	0.29	0.13	0.21	0.29
o2	0.47	0.15	0.04	0.38	0.36	0.18	0.25	0.28	0.11	0.28	0.19	0.20
F7	0.13	0.20	0.13	0.14	0.26	0.08	0.15	0.12	0.03	0.01	0.22	0.19
F8	0.11	0.04	0.25	0.08	0.20	0.18	0.12	0.34	0.27	0.08	0.12	0.01
T3	0.03	0.32	0.07	0.29	0.20	0.05	0.35	0.14	0.17	0.12	0.54	0.12
T4	0.00	0.08	0.31	0.16	0.29	0.08	0.12	0.39	0.11	0.08	0.15	0.37
T5	0.18	0.50	0.04	0.06	0.34	0.00	0.35	0.44	0.17	0.04	0.42	0.04
T6	0.34	0.18	0.46	0.35	0.03	0.45	0.32	0.29	0.10	0.01	0.16	0.10
Fz	0.26	0.10	0.08	0.19	0.05	0.31	0.10	0.06	0.09	0.30	0.10	0.18
Cz	0.24	0.17	0.23	0.12	0.14	0.41	0.09	0.09	0.09	0.00	0.10	0.12
Pz	0.12	0.20	0.35	0.06	0.12	0.11	0.04	0.12	0.10	0.58	0.07	0.36
Average	0.1974	0.1878	0.1885	0.1935	0.1997	0.1865	0.1899	0.1837	0.1876	0.1647	0.1786	0.2065

Once the previous step has been carried out, loads which are higher than the mentioned average is compared, the number of times they are higher

than the average is counted, first, up to component 12 and then up to component 8, and from there those with higher quantity in common are the channels chosen, since they are the channels with the greatest relevance (table 4). This procedure is followed because up to component 12, 95% accumulates, but the first 8 PCs are the ones which have the greatest weight, since with them 91% is reached, while in PCs 9,10,11 and 12, even when they are higher than average, however, they have less weight compared to the first 8.

Table 4: Matrix With Above Average Channel Selection And Summary Of Comparison Between PCA 12 And PCA 8 For Each Movement And Healthy Subject.

	PC1	PC2	PC3	PC4	PC5	PC6	PC7	PC8	CP9	PC10	PC11	PC12	COUNT 12	COUNT 8
FP1	YES	NO	YES	NO	YES	YES	YES	YES	YES	NO	NO	YES	8	6
FP2	YES	NO	YES	YES	NO	YES	NO	NO	NO	YES	NO	YES	6	4
F3	YES	NO	NO	NO	YES	NO	NO	NO	YES	YES	NO	YES	5	2
F4	YES	NO	NO	YES	NO	NO	NO	NO	NO	NO	NO	YES	3	2
C3	NO	NO	YES	YES	YES	NO	NO	YES	NO	NO	YES	NO	5	4
C4	NO	YES	NO	YES	YES	YES	YES	NO	YES	NO	YES	NO	7	5
P3	YES	YES	YES	NO	NO	YES	YES	NO	NO	NO	YES	YES	7	5
P4	YES	YES	NO	NO	YES	YES	NO	YES	YES	YES	NO	YES	8	5
O1	YES	YES	NO	YES	YES	NO	NO	NO	YES	NO	YES	YES	7	4
o2	YES	NO	NO	YES	YES	NO	YES	YES	NO	YES	YES	YES	8	5
F7	NO	YES	NO	NO	YES	NO	NO	NO	NO	NO	YES	NO	3	2
F8	NO	NO	YES	NO	NO	NO	NO	YES	YES	NO	NO	NO	3	2
T3	NO	YES	NO	YES	NO	NO	YES	NO	NO	NO	YES	NO	4	3
T4	NO	NO	YES	NO	YES	NO	NO	YES	NO	NO	NO	YES	4	3
T5	NO	YES	NO	NO	YES	NO	YES	NO	NO	NO	YES	NO	5	4
T6	YES	YES	YES	YES	NO	YES	YES	YES	NO	NO	NO	NO	7	7
Fz	YES	NO	NO	NO	NO	YES	NO	NO	NO	YES	NO	NO	3	2
Cz	YES	NO	YES	NO	NO	YES	NO	NO	NO	NO	NO	NO	3	3
Pz	NO	YES	YES	NO	NO	NO	NO	NO	YES	NO	YES	NO	4	2

To individually select which channel has greater weight than the other, the number of common repetitions between PCA 8 and PCA 12 is analyzed. If the figures are similar between both and greater than 4, this channel provides useful and necessary information, if in Change has much more quantity in PCA 12 than in PCA 8, this channel does not present much information because it is the last components that present relevance and do not give much explained variability. Table 5 illustrates such a procedure in the patients designated as 22 GDR and 18 DCA, showing those channels that provide significant information.

Table 5: Summary Of Comparison Between PCA 12 And PCA 8 For Each Movement And Healthy Subject

Channels	22DGR						18AD					
	FirstMovement		SecondMovement		ThirdMovement		FirstMovement		SecondMovement		ThirdMovement	
	PCA 8	PCA 4	PCA 8	PCA 4	PCA 8	PCA 4	PCA 8	PCA 4	PCA 8	PCA 4	PCA 8	PCA 4
FP1	3	0	3	0	1	0	3	2	5	2	4	2
FP2	1	0	2	0	1	0	4	2	4	2	3	2
F3	2	1	2	1	2	1	2	1	2	1	3	2
F4	0	0	0	0	0	0	1	1	4	2	3	3
C3	4	2	3	2	4	2	4	2	5	2	4	2
C4	5	2	6	3	4	2	5	2	4	2	6	2
P3	3	2	3	2	3	2	4	2	4	2	5	3
P4	4	2	4	2	4	2	6	3	6	3	6	3
O1	4	3	4	3	5	3	6	4	5	3	7	4
O2	7	3	4	3	7	3	5	3	6	3	5	3
F7	3	2	3	1	3	1	4	2	4	3	3	2
F8	2	0	2	0	2	0	1	0	1	0	2	1
T3	3	2	4	2	5	3	4	2	3	1	3	2
T4	3	1	3	1	3	1	0	0	0	0	0	0
T5	5	2	5	2	6	3	4	1	3	1	4	1
T6	6	3	6	3	6	3	4	1	4	1	4	1
Fz	2	1	2	1	2	0	2	2	1	1	2	2
Cz	4	3	4	2	5	2	4	2	3	2	4	1
Pz	2	2	2	2	3	2	4	2	4	3	4	2

Subsequently, the average of the number of components that exceeded the mean is performed up to the components indicated in each movement for each patient and the average of the number of components that exceeded the average among all the movements. To that reflected in the previous figure for the individual selection of each channel it was compared in a similar way, but this time in a general way (Table 6).

Table 6: General Summary Of Movements, PCA And Channels.

First Movement	PCA 12		PCA 8		Third Movement		PCA 12	PCA 8	Channels
	PCA 12	PCA 8	PCA 12	PCA 8	PCA 12	PCA 8			
4	2	4,375	1,875	4,25	1,875	4.20833333	1.91666667	FP1	
3,25	2	3,75	1,75	3,125	1,75	3,375	1,83333333	FP2	
2,875	1,375	3,25	1,375	3,625	1,5	3,25	1,41666667	F3	
2,5	1	2,5	1,25	3	1,625	2,66666667	1,29166667	F4	
2,75	1,75	2,875	1,5	3	1,625	2,875	1,625	C3	
4,125	2,125	3,375	2,125	3,875	2,125	3,79166667	2,125	C4	
3	2	3,375	2,125	3,25	2	3,20833333	2,04166667	P3	
3,875	2,25	4	2,125	4,375	2,25	4,08333333	2,20833333	P4	
4,125	2,75	4,5	2,625	4,5	2,625	4,375	2,66666667	O1	
4,75	2,375	4,875	2,625	5	2,75	4,875	2,58333333	o2	
4,25	2	4,125	2,125	4,375	2,125	4,25	2,08333333	F7	
2,125	0,25	2,75	0,375	2,625	0,5	2,5	0,375	F8	
3,5	1,625	3,625	1,625	3,625	2,125	3,58333333	1,79166667	T3	
2	0,5	2,75	0,875	2,25	0,625	2,33333333	0,66666667	T4	
4,5	2,125	4,875	2,25	5	2,25	4,79166667	2,20833333	T5	
4,875	2,125	4,375	2,125	4,625	2	4,625	2,08333333	T6	
2,25	1,625	2,375	1,5	2	1,125	2,20833333	1,41666667	Fz	
3,25	1,75	3,25	1,75	3	1,625	3,16666667	1,70833333	Cz	
2,75	1,75	3,125	2	3,25	1,875	3,04166667	1,875	Pz	

Once the procedure described above was carried out, the results obtained were that the channels with the greatest information at the frequency of the alpha brain rhythm are the following: FP1, FP2, C4, P4, O1, O2, F7, T3, T5, T6 and Cz, and for the beta brain rhythm: FP1, FP2, F3, F4, C3, C4, O1, O2, F7, T3, T4, T5, T6 and Cz. The FP1 and FP2 channels were eliminated because each patient was stimulated visually, so they have visual information, which makes them not useful for the study. These results were validated by a specialist in neurophysiology, and later, according to the bibliography studied, the study focused only on the C3, C4 and Cz channels, since they are the ones

found in the premotor area and central fissure, where the primary motor cortex, which is the area responsible for allowing the generation, maintenance, and termination of voluntary and conscious movements.

3.4 Fourier Transform

Once the dimensionality of the database has been reduced using PCA, it becomes imperative to create some algorithm or procedure that allows determining or differentiating the movements made. The Fourier Transform was used, one of the most widely used procedures in electroencephalography, since it allows analyzing the signals from the point of view of frequency. The latter is relevant because each amplitude, each band or brain rhythm reflects a type of movement or type of processing.

Figure 12 shows the results of the DFT in the C3 channel and in the Alpha channel (flexion-extension movement) for patient 22DGR, a procedure that was carried out for each subject, movement and brain rhythm.

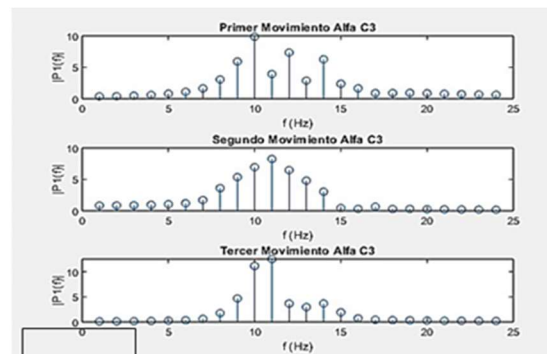


Figure 12: DFT Of Patient 22DGR. Channel C3 Brain Rhythm Alpha.

Although there were differentiating characteristics among the samples, a common base frequency or amplitude to all of them was not verified. The frequency in a certain rhythm or channel presented differently itself. In this sense, it was decided to practice the procedure for each of the repetitions of the different channels and brain rhythms of each of the subjects. As can be seen, no common characteristic was found (Figure 13).

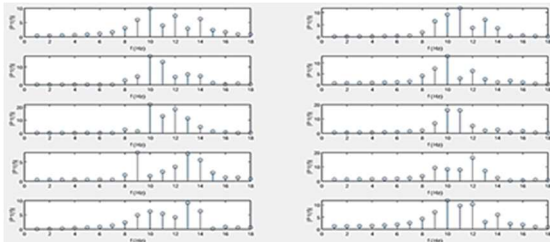


Figure 13: Analysis Of The DFT For Each Of The Repetitions Of The Patient 22DGR, Channel C3 Brain Rhythm Alpha.

Figure 14 reinforces this last criterion. As observed based on the mean of all the repetitions for each subject, the amplitude of the mean vector of the repetitions, there are no common neighboring points in each channel and movement that allow to identify the type of movement.

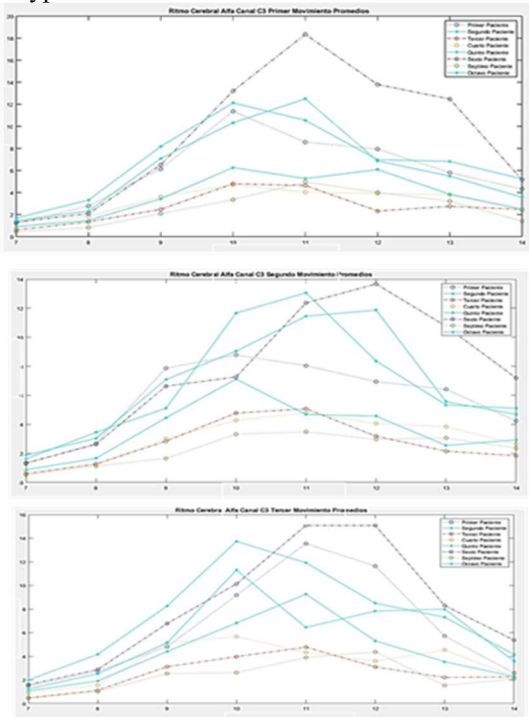


Figure 14: DFT Of Each Of The Patients In Channel C3 Brain Alpha Rhythm Executing The Extension Movement. (B) Abduction-Adduction. (C) Flexion-Extension.

With these inconclusive results in the use of the DFT to the complete signal or to each one of the repetitions of the exercises, it was decided to carry out the Fast Fourier Transform (FFT).

For this, multiples of the sampling frequency were chosen as the length of the window of the signal to perform the FFT and the displacement of the window, because the duration of the number of samples of each of the parts on each repetition of an exercise are integer multiples of that

frequency. Subsequently, a Hamming-type window of the size of the length of the window to perform the FFT was designed, and the number of segments in which the mentioned procedure will be performed is calculated [25]. Once this was done, the signal to which the algorithm is performed, the segment that is processed, the transform of the mentioned segment and the spectrogram were simultaneously displayed on a graph. In case of having performed a repetition of a complete exercise, it was displayed the spectrogram of the repetition.

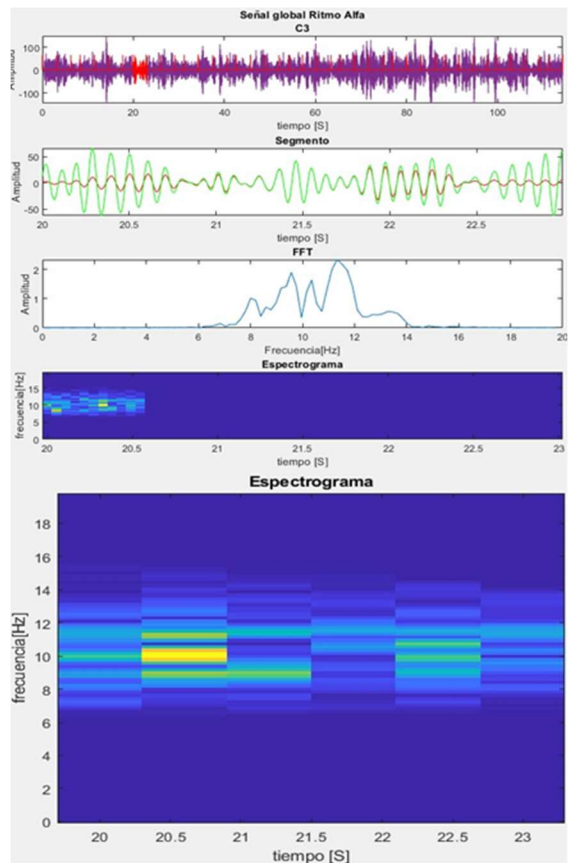


Figure 15: Graph Of The Signal To Which The FFT Is Applied, As Well As The FFT Spectrogram.

With the application of the fast Fourier transform it was possible to determine that approximately one second before the performance of each exercise, a fundamental frequency is identified which constitutes an indicator of the imminent execution of a movement. The spectrogram showed this mark for each sample taken, so by applying the FFT it is possible to determine when a movement will take place (figure 14). In most of the cases studied, the frequency of said movement varies according to the patient in the beta cerebral rhythm, even so, it was possible to determine that for the first

movement in the alpha cerebral rhythm the central frequency is 10 Hz, however, in the second and third movements in the alpha brain rhythm the center frequency is 11 Hz.

Figure 16 shows how 1 s before the execution of the movement there is a determining frequency.

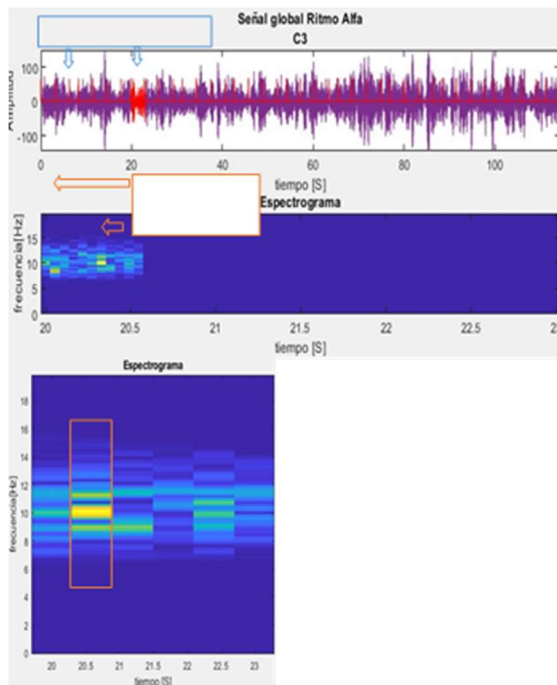


Figure 16: Existence Of A Determining Frequency 1 S Before The Execution Of The Movement.

#### 4. CONCLUSIONS

The present work proposes a methodology that includes the recognition of the intention of real movements included in therapeutic programs of rehabilitation of the upper limb. The developed instrument allows to determine the type of movement, beginning, duration and end of each one of them, the extraction of the signal, prior to the classification methods as part of an active brain-computer interface system. As a flexible tool other signal extraction method could be incorporated.

#### REFERENCES:

- [1] Anuario Estadístico de América Latina y el Caribe, Publicación de las Naciones Unidas / United Nations publication., n° ISBN: 978-92-1-121880-0 (versión impresa y pdf) / (print and pdf). ISBN: 978-92-1-057208-8 (versión ePub) / (ePub). 2013.
- [2] Anuario Estadístico de América Latina y el Caribe Publicación de las Naciones Unidas / United Nations publication., n° ISBN: 978-92-1-121880-0 (versión impresa y pdf) / (print and pdf). ISBN: 978-92-1-057208-8 (versión ePub) / (ePub).2014.
- [3] W. H. Organization., "Recommendations on stroke prevention, diagnosis, and therapy", Report of the WHO Task Force on Stroke and other Cerebrovascular Disorders., n° 20, pp. 1407-1431.
- [4] C. I. Puentes Madera, "Epidemiología de las enfermedades cerebrovasculares de origen extracranial.", Revista cubana de Angiol Circ. Vas., vol. 15, n° 2, pp. 74-83, 2014.
- [5] Anuario estadístico de salud año 2021, La Habana, 2021. Disponible en línea <http://www.who.int.Classification/icd/icd10usupdates/en>.
- [6] C. R. Boninger ML. "Why do we need improved mobility technology?". J Neuro Eng and rehabilitation 2012,9:16, <http://jneuroengrehab.com/content/9/1/16>
- [7] J. J. Vidal, "Toward direct brain-computer communication". Annual review of biophysics and bioengineering, vol. 2, pp. 157-180, 1973.
- [8] R. Wolpaw, N. Birbaumer, D. J. McFarland, G. Pfurtscheller y T. M. Vaughan, "Braincomputer interfaces for communication and control". Clinical Neurophysiology, vol. 113, n° 6, pp. 767-791, 2002.
- [9] B. Kleber y N. Birbaumer, "Direct brain communication: neuroelectric and metabolic approaches at Tübingen". Cognitive Processing, vol. 6, n° 1, pp. 65-74, 2005.
- [10] I. S. Kotchetkov, B. Y. Hwang, G. Appelboom, C. P. Kellner y E. S. Connolly Jr, "Brain-computer interfaces: military, neurosurgical, and ethical perspective". Neurosurgical Focus, vol.28, n° 5, 2010.
- [11] Jin J., Zhang H., Daly I., Wang X. y Cichocki A., "An improved P300 pattern in BCI to catchuser's attention" Journal Neural Engineering, 2017.
- [12] M. Soufneyestani, "Electroencephalography (EEG) Technology Applications and Available Devices" Appl. Science, n° 10, 2020.
- [13] Azorin, J.M et al."La Interacción de Personas con Discapacidad con el Computador: Experiencias y Posibilidades en Iberoamérica". Editorial Programa Iberoamericano de Ciencia y Tecnología para el Desarrollo (CYTED), ISBN-10: 84-15413-22-X, 2013.
- [14] Neta Rabin et al. "Classification of human hand movements based on EMG signals using nonlinear dimensionality reduction and data

- fusion techniques”. *Expert Systems with Applications* 149 (2020) 113281.
- [15] Al-Angari, H. M., Kanitz, G., Tarantino, S., & Cipriani, C. . “Distance and mutual information methods for EMG feature and channel subset selection for classification of hand movements”. *Biomedical Signal Processing and Control*, 27, 24-31.2016.
- [16] Dsilva, C. J., Talmon, R., Coifman, R. R., & Kevrekidis, I. G. “Parsimonious representation of nonlinear dynamical systems through manifold learning: A chemotaxis case study”. *Applied and Computational Harmonic Analysis*, 44(3), 759-773.2018.
- [17] M. A. Lopez. “Interfaz ICCS de altas prestaciones basada en la detección y procesamiento de la actividad cerebral”. Tesis doctorada, repositorio, Universidad de Granadas, 2009.
- [18] J. de la O. Chavez. “Interfaz cerebro-computadora para el control de un cursor basada en ondas cerebrales”. Tesis doctorada. Universidad Autónoma Metropolitana Azcapotzalco, México 2006.
- [19] T. Eichele y col. “Removal of MRI artifacts from EEG recordings”. *Simultaneous EEG and fMRI: Recording, Analysis, and Application*. Ed. M. Ullsperger y S. Debener. Oxford Scholarship. Cap. 2-3.2010.
- [20] B. Blankertz y col. “Invariant common spatial patterns: Alleviating nonstationarities in brain computer interfacing”. *Advances in Neural Information Processing Systems* 20 .2008.
- [21] L. Roijendijk. “Variability and nonstationarity in Brain Computer Interfaces”. Tesis de licenciatura. Radboud University Nijmegen, 2009.
- [22] M. Poulos y col. “On the use of EEG features towards person identification via neural networks”. En: *Medical Informatics and the Internet in Medicine* 26.1, págs. 35-48.1999.
- [23] Mahsa Soufineyestani et al. *Electroencephalography (EEG) Technology Applications and Available Devices*. *Appl. Sci.* 2020, 10, 7453; doi:10.3390/app10217453
- [24] Andrea Valenti et al.” A Deep Classifier for Upper-Limbs Motor Anticipation Tasks in an Online BCI Setting”. *Bioengineering*. 2021, 8, 21.  
<https://doi.org/10.3390/bioengineering8020021>.
- [25] Jaime Delgado Saa et al.”Using Coherence-based spectrospatial filters for stimulus features prediction from electrocorticographic recordings”. *Scientific Reports*. 2020 10:7637 | <https://doi.org/10.1038/s41598-020-63303-1>.
- [26] Cachaya, E. S. U., Perdomo, C. A. P., Suaza, D. M. E., Zarta, J. B. R., & Serrezuela, R. R. (2024). Control of Autonomous Motorcycles by Means of Trajectory Tracking and Balance Stabilization. *Journal of Theoretical and Applied Information Technology*, 102(7).
- [27] Buelvas, H. E. P., Montaña, J. D. T., & Serrezuela, R. R. (2023). Hand Gesture Classification using Deep learning and CWT images based on multi-channel surface EMG signals. In *2023 3rd International Conference on Electrical, Computer, Communications and Mechatronics Engineering (ICECCME)* (pp. 1-7). IEEE.

Table 1: Eigenvalue matrix

	PC1	PC2	PC3	PC4	PC5	PC6	PC7	PC8	CP9	PC10	PC11	PC12
FP1	-0.22	0.09	0.20	-0.19	-0.34	-0.26	0.23	0.41	0.33	0.14	-0.04	-0.22
FP2	-0.20	0.00	0.21	-0.26	-0.03	-0.21	0.18	0.10	-0.11	0.19	-0.05	0.26
F3	-0.22	0.06	-0.04	0.03	-0.25	0.15	-0.06	-0.06	0.20	-0.51	-0.20	-0.19
F4	-0.21	-0.08	0.09	-0.22	0.09	-0.01	0.02	0.00	-0.16	-0.08	0.03	0.38
C3	-0.09	0.12	-0.29	0.42	-0.22	0.12	0.15	-0.25	0.13	0.12	-0.48	0.16
C4	-0.03	-0.35	-0.08	0.21	0.37	-0.36	-0.30	0.01	0.59	-0.02	0.08	0.24
P3	0.22	0.19	-0.45	0.07	0.02	-0.20	0.54	-0.01	-0.10	-0.14	0.20	0.26
P4	0.34	-0.42	-0.14	0.06	-0.24	-0.35	-0.15	0.24	-0.40	-0.30	-0.05	-0.21
O1	0.34	0.30	-0.13	-0.40	0.26	0.04	0.09	-0.16	0.29	-0.13	0.21	-0.29
o2	0.47	-0.15	0.04	-0.38	-0.36	0.18	-0.25	-0.28	0.11	0.28	-0.19	0.20
F7	-0.13	0.20	0.13	0.14	-0.26	-0.08	-0.15	-0.12	0.03	0.01	0.22	-0.19
F8	-0.11	-0.04	0.25	-0.08	0.20	-0.18	0.12	-0.34	-0.27	0.08	-0.12	0.01
T3	-0.03	0.32	0.07	0.29	-0.20	-0.05	-0.35	-0.14	-0.17	0.12	0.54	0.12
T4	0.00	-0.08	0.31	0.16	0.29	-0.08	0.12	-0.39	-0.11	-0.08	-0.15	-0.37
T5	0.18	0.50	0.04	0.06	0.34	0.00	-0.35	0.44	-0.17	0.04	-0.42	0.04
T6	0.34	-0.18	0.46	0.35	0.03	0.45	0.32	0.29	0.10	-0.01	0.16	0.10
Fz	-0.26	-0.10	-0.08	-0.19	0.05	0.31	-0.10	0.06	-0.09	-0.30	0.10	0.18
Cz	-0.24	-0.17	-0.23	-0.12	0.14	0.41	-0.09	0.09	-0.09	0.00	0.10	-0.12
Pz	-0.12	-0.20	-0.35	0.06	0.12	0.11	0.04	0.12	-0.10	0.58	0.07	-0.36

Table 3: Matrix of Absolute Eigenvalues.

Matrix of Absolute Eigenvalues												
	PC1	PC2	PC3	PC4	PC5	PC6	PC7	PC8	CP9	PC10	PC11	PC12
FP1	0.22	0.09	0.20	0.19	0.34	0.26	0.23	0.41	0.33	0.14	0.04	0.22
FP2	0.20	0.00	0.21	0.26	0.03	0.21	0.18	0.10	0.11	0.19	0.05	0.26
F3	0.22	0.06	0.04	0.03	0.25	0.15	0.06	0.06	0.20	0.51	0.20	0.19
F4	0.21	0.08	0.09	0.22	0.09	0.01	0.02	0.00	0.16	0.08	0.03	0.38
C3	0.09	0.12	0.29	0.42	0.22	0.12	0.15	0.25	0.13	0.12	0.48	0.16
C4	0.03	0.35	0.08	0.21	0.37	0.36	0.30	0.01	0.59	0.02	0.08	0.24
P3	0.22	0.19	0.45	0.07	0.02	0.20	0.54	0.01	0.10	0.14	0.20	0.26
P4	0.34	0.42	0.14	0.06	0.24	0.35	0.15	0.24	0.40	0.30	0.05	0.21
O1	0.34	0.30	0.13	0.40	0.26	0.04	0.09	0.16	0.29	0.13	0.21	0.29
o2	0.47	0.15	0.04	0.38	0.36	0.18	0.25	0.28	0.11	0.28	0.19	0.20
F7	0.13	0.20	0.13	0.14	0.26	0.08	0.15	0.12	0.03	0.01	0.22	0.19
F8	0.11	0.04	0.25	0.08	0.20	0.18	0.12	0.34	0.27	0.08	0.12	0.01
T3	0.03	0.32	0.07	0.29	0.20	0.05	0.35	0.14	0.17	0.12	0.54	0.12
T4	0.00	0.08	0.31	0.16	0.29	0.08	0.12	0.39	0.11	0.08	0.15	0.37
T5	0.18	0.50	0.04	0.06	0.34	0.00	0.35	0.44	0.17	0.04	0.42	0.04
T6	0.34	0.18	0.46	0.35	0.03	0.45	0.32	0.29	0.10	0.01	0.16	0.10
Fz	0.26	0.10	0.08	0.19	0.05	0.31	0.10	0.06	0.09	0.30	0.10	0.18
Cz	0.24	0.17	0.23	0.12	0.14	0.41	0.09	0.09	0.09	0.00	0.10	0.12
Pz	0.12	0.20	0.35	0.06	0.12	0.11	0.04	0.12	0.10	0.58	0.07	0.36
Average	0.1974	0.1878	0.1885	0.1935	0.1997	0.1865	0.1899	0.1837	0.1876	0.1647	0.1786	0.2065

Table 4: Matrix with above average channel selection and Summary of comparison between PCA 12 and PCA 8 for each movement and healthy subject.

Matrix of Absolute Values Above the Mean														
	PC1	PC2	PC3	PC4	PC5	PC6	PC7	PC8	CP9	PC10	PC11	PC12	COUNT 12	COUNT 8
FP1	YES	NO	YES	NO	YES	YES	YES	YES	YES	NO	NO	YES	8	6
FP2	YES	NO	YES	YES	NO	YES	NO	NO	NO	YES	NO	YES	6	4
F3	YES	NO	NO	NO	YES	NO	NO	NO	YES	YES	YES	NO	5	2
F4	YES	NO	NO	YES	NO	NO	NO	NO	NO	NO	NO	YES	3	2
C3	NO	NO	YES	YES	YES	NO	NO	YES	NO	NO	YES	NO	5	4
C4	NO	YES	NO	YES	YES	YES	YES	NO	YES	NO	NO	YES	7	5
P3	YES	YES	YES	NO	NO	YES	YES	NO	NO	NO	YES	YES	7	5
P4	YES	YES	NO	NO	YES	YES	NO	YES	YES	YES	NO	YES	8	5
O1	YES	YES	NO	YES	YES	NO	NO	NO	YES	NO	YES	YES	7	4
o2	YES	NO	NO	YES	YES	NO	YES	YES	NO	YES	YES	YES	8	5
F7	NO	YES	NO	NO	YES	NO	NO	NO	NO	NO	YES	NO	3	2
F8	NO	NO	YES	NO	NO	NO	NO	YES	YES	NO	NO	NO	3	2
T3	NO	YES	NO	YES	NO	NO	YES	NO	NO	NO	YES	NO	4	3
T4	NO	NO	YES	NO	YES	NO	NO	YES	NO	NO	NO	YES	4	3
T5	NO	YES	NO	NO	YES	NO	YES	YES	NO	NO	YES	NO	5	4
T6	YES	YES	YES	YES	NO	YES	YES	YES	NO	NO	NO	NO	7	7
Fz	YES	NO	NO	NO	NO	YES	NO	NO	NO	YES	NO	NO	3	2
Cz	YES	NO	YES	NO	NO	YES	NO	NO	NO	NO	NO	NO	3	3
Pz	NO	YES	YES	NO	NO	NO	NO	NO	NO	YES	NO	YES	4	2

Table 5: Summary of comparison between PCA 12 and PCA 8 for each movement and healthy subject

Channels	22DGR						18AD					
	First Movement		Second Movement		Third Movement		First Movement		Second Movement		Third Movement	
	PCA 8	PCA 4	PCA 8	PCA 4	PCA 8	PCA 4	PCA 8	PCA 4	PCA 8	PCA 4	PCA 8	PCA 4
FP1	3	0	3	0	1	0	3	2	5	2	4	2
FP2	1	0	2	0	1	0	4	2	4	2	3	2
F3	2	1	2	1	2	1	2	1	2	1	3	2
F4	0	0	0	0	0	0	1	1	4	2	3	3
C3	4	2	3	2	4	2	4	2	5	2	4	2
C4	5	2	6	3	4	2	5	2	4	2	6	2
P3	3	2	3	2	3	2	4	2	4	2	5	3
P4	4	2	4	2	4	2	6	3	6	3	6	3
O1	4	3	4	3	5	3	6	4	5	3	7	4
o2	7	3	4	3	7	3	5	3	6	3	5	3
F7	3	2	3	1	3	1	4	2	4	3	3	2
F8	2	0	2	0	2	0	1	0	1	0	2	1
T3	3	2	4	2	5	3	4	2	3	1	3	2
T4	3	1	3	1	3	1	0	0	0	0	0	0
T5	5	2	5	2	6	3	4	1	3	1	4	1
T6	6	3	6	3	6	3	4	1	4	1	4	1
FZ	2	1	2	1	2	0	2	2	1	1	2	2
CZ	4	2	4	2	5	2	4	2	3	2	4	1
CP	2	2	2	2	3	2	4	2	4	3	4	2

Table 6: General Summary of Movements, PCA and Channels.

First Movement		Second Movement		Third Movement		PCA 12	PCA 8	Channels
PCA 12	PCA 8	PCA 12	PCA 8	PCA 12	PCA 8			
4	2	4,375	1,875	4.25	1,875	4.20833333	1.91666667	FP1
3.25	2	3.75	1.75	3,125	1.75	3,375	1.83333333	FP2
2,875	1,375	3.25	1,375	3,625	1.5	3.25	1.41666667	F3
2.5	1	2.5	1.25	3	1,625	2.66666667	1.29166667	F4
2.75	1.75	2,875	1.5	3	1,625	2,875	1,625	C3
4,125	2,125	3,375	2,125	3,875	2,125	3.79166667	2,125	C4
3	2	3,375	2,125	3.25	2	3.20833333	2.04166667	P3
3,875	2.25	4	2,125	4,375	2.25	4.08333333	2.20833333	P4
4,125	2.75	4.5	2,625	4.5	2,625	4,375	2.66666667	O1
4.75	2,375	4,875	2,625	5	2.75	4,875	2.58333333	o2
4.25	2	4,125	2,125	4,375	2,125	4.25	2.08333333	F7
2,125	0.25	2.75	0.375	2,625	0.5	2.5	0.375	F8
3.5	1,625	3,625	1,625	3,625	2,125	3.58333333	1.79166667	T3
2	0.5	2.75	0.875	2.25	0.625	2.33333333	0.66666667	T4
4.5	2,125	4,875	2.25	5	2.25	4.79166667	2.20833333	T5
4,875	2,125	4,375	2,125	4,625	2	4,625	2.08333333	T6
2.25	1,625	2,375	1.5	2	1,125	2.20833333	1.41666667	Fz
3.25	1.75	3.25	1.75	3	1,625	3.16666667	1.70833333	Cz
2.75	1.75	3,125	2	3.25	1,875	3.04166667	1,875	Pz